Primljen / Received: 13.5.2022.
Ispravljen / Corrected: 13.1.2023.
Prihvaćen / Accepted: 28.4.2023.
Dostupno online / Available online: 10.7.2023.

Numerical and experimental analyses of a steel "Y" joint with damage

Authors:

Marko Milošević, MSc. CE
University of Niš, Serbia
Faculty of Civil Engineering
marko.milosevic.mat@gmail.com
Corresponding author

Prof. **Dragoslav Stojić**, PhD. CE
University of Niš, Serbia
Faculty of Civil Engineering
dragoslav.stojic@gaf.ni.ac.rs

Assoc.Prof. **Srđan Živković**, PhD. CE
University of Niš, Serbia
Faculty of Civil Engineering
srdjan.zivkovic@gaf.ni.ac.rs

Assist.Prof. **Dragan S. Jovanović**, PhD. Mach
University of Niš, Serbia
Faculty of Civil Engineering
dragan.s.jovanovic@masfak.ni.ac.rs

Research Paper

Marko Milošević, Dragoslav Stojić, Srđan Živković, Dragan S. Jovanović

Numerical and experimental analyses of a steel "Y" joint with damage

Steel damage can significantly impact steel elements' performance, affecting other structural and non-structural building parts and compromising safety and functioning. Understanding the processes and mechanisms of steel structure damage is crucial for improving its durability. This paper presents numerical and experimental analyses of type "Y" joint behaviour of truss beams in a plane loaded by an axial force, with a special accent on the damage effects. This paper presents the results of numerical and experimental research on the directly welded Y joint of the SHS chord and diagonal members with damage in the joint in the form of a narrow vertical rectangular crack. The deviation of the results obtained by the numerical and experimental procedures was, on average 3 % to 5 %.

Key words:
experimental analysis, numerical analysis, steel joints, Y joint, truss beams, RHS and SHS sections

Prethodno priopćenje

Marko Milošević, Dragoslav Stojić, Srđan Živković, Dragan S. Jovanović

Numerička i eksperimentalna analiza čeličnog "Y" priključka s oštećenjima

Oštećenje čelika može značajno utjecati na performanse čeličnih elemenata, utječući na druge konstrukcijske i nekonstrukcijske dijelove zgrade i ugrožavajući sigurnost i funkcioniranje. Razumijevanje procesa i mehanizama oštećenja čelične konstrukcije ključno je za poboljšanje njezine trajnosti. U ovom su radu prikazane numeričke i eksperimentalne analize ponašanja "Y" priključaka rešetkastih nosača u ravnini opterećenih uzdužnom silom, s posebnim naglaskom na učinke oštećenja. U ovom su radu prikazani rezultati numeričkih i eksperimentalnih istraživanja izravno zavarenog Y priključka SHS pojasnog štapa i dijagonalnih elemenata s oštećenjem priključka u obliku uske vertikalne pravokutne pukotine. Odstupanje rezultata dobivenih numeričkim i eksperimentalnim postupcima iznosilo je u prosjeku 3 % do 5 %.

Ključne riječi:
eksperimentalna analiza, numerička analiza, čelični priključci, Y priključak, rešetkaste grede, RHS i SHS presjeci

1. Introduction

Truss beams of hollow steel sections are widely used in civil engineering for building and bridge construction [1]. They are frequently used as roof supports, purlins, floor beams, and crane supports in industrial halls, sports buildings, congress halls, exhibition pavilions, and high-rise structures. They are commonly used due to multiple advantages, such as high load-bearing capacity, low aerodynamic coefficient, quick and easy assembly, potential use in internal spaces in installations and lines, low cost of anti-corrosive protection, cost-effectiveness, and high susceptibility to creative structural and architectural design. Such truss beams also have disadvantages, such as the additional work (especially for truss beams made of hollow circular cross–sections) and higher unit costs than that of hot-rolled sections.

The advantages of using square and rectangular hollow sections for the joints of truss beams with directly welded elements compared to circular pipes are indisputable, as reflected in the formal and structural advantages (straight cutting), simplicity, and optional stiffeners of the flange plates and side plates.

Generally, the joints of truss girder elements can be either direct or indirect. A direct joint is characterised by brace members directly welded to the chord of the element. These joints can be either reinforced or non-reinforced. In an indirect joint, the chord and brace members are mutually joined via gusset plates using rivets, bolts, or welding. The transmission of forces of the direct joint (as suggested by its name) is direct, from one element to the other; in the case of an indirect joint, the transmission is longer because the force is first transmitted to the gusset plate and then from the gusset plate onto the other element. Certainly, the direct joint should take precedence because, in statistical terms, the potential for error is twice as low. At the same time, the local buckling of the chord cross-sectional flange at the joint owing to the introduction of force via the gusset plate should not be ignored.

Damage may occur to the parts of steel structures and their joints during service because of insufficient or inadequate maintenance. Damage can differ from mechanical damage caused by overload or impact in the form of cracks or deterioration caused by chemical or biological long-term corrosive action. This damage can reduce the structural bearing capacity, damage other structural and non-structural parts of buildings, and compromise the functionality and safety of the structure. Understanding the causes and effects of damage as well as the damage processes, mechanisms, and propagation, is important for the service life of steel structures.

This paper presents experimental and numerical analyses on models with and without damage of type "Y" joints of truss beams in a plane loaded by an axial force during static loading. The model includes an initial "small" vertical crack in the shape of a narrow rectangle that is 15 mm high. Afterwards, this damage propagates along the height of the chord member with incremental steps of 15 mm until it reaches a final size of 60 mm (Figure 5).

In practice, during the monitoring of structures, possibly when damage is detected as a "small" crack in the truss node, it increases in size over time.

2. Review of regulations and research

2.1. Technical regulations

The current regulations for the design of metal structures in Europe are EN 1993-1-1 (*Eurocode 3: Design of steel structures – Part 1-1: General rules and rules for building*) [2] and EN 1993-1-8 (*Eurocode 3: Design of steel structures – Part 1-8: Design of joints*) [3].

2.2. Theoretical research

The master's thesis [4] provides an in-depth review of all rules for determining the design ultimate resistance of joints according to EC3, both plane and space frame truss beams, loaded by an axial force and/or by the bending moment. These formulations are graphically illustrated and accompanied by adequate numerical examples, which are particularly important for rapidly determining resistance in the initial design phases. In addition to joints made of hollow rectangular sections, the author analysed other types of joints (made of hollow rectangular, square, and tubular sections, as well as I, H, and U sections).

In the framework of CIDECT, papers [5, 6] have been published dealing with the theoretical principles of the design of directly welded joints made of hollow sections. These publications provided recommendations for designing this type of joint.

The authors in [7] updated the results and rules for designing directly welded joints of hollow sections and described the changes, advances, expansions, and recommendations. Two new CIDECT guidelines for joint design were presented.

Recently, [8] was published to review the recent research on hollow section joints of welded high-strength steel (HSS). This paper describes the standing design rules for directly welded joints of high-strength steel and summarises recent research in this field.

2.3. Experimental research

Experimental research on the behaviour of directly welded joints of truss beam elements made of hollow rectangular and square steel sections was analysed in a PhD thesis [9]. The author, in his doctoral thesis, acquired the relevant results using analytical and numerical procedures implemented on models of type "T" and "Y" joints and by obtaining experimental confirmation of the results, on whose bases the conclusions about the effects of various parameters on the behaviour of these types of joints were drawn. The author also demonstrated that the load-bearing capacity of experimentally tested joints is exhausted owing to the local plasticisation of the flange surface of the chord member; the joint exhibits elastoplastic behaviour with

a prominent elastic deformation, and the effect of plasticisation of the side walls on the ultimate resistance is negligible. This study is a continuation of the research initiated in this doctoral dissertation. The principles and parameters used in this doctoral dissertation served as the basis for planning the experiments in this study.

2.4. Numerical research

In [10], the results of parametric research on the static strength of in-plane bending-loaded tubular "T" joints with a reinforced chord were presented. The aforementioned research, conducted using non-linear finite elements, indicated that the sidewall thickness of the chord member significantly impacted the total bearing capacity of the T-joints, influencing the geometry definition of the tested models in this study.
Marcel Garifullin and a group of authors also contributed to the behaviour of "T" joints of directly welded hollow rectangular sections. In the study [11], the authors developed a finite element model of a "T" joint of high-grade steel, loaded by axial forces and bending moment in a plane. Based on the results of a series of experimental tests, the authors provided recommendations for choosing the optimal type of finite element. In the study [12], the componential method for modelling "T" joints of hollow sections under axial forces and moments in a plane was researched using a combination of springs and a proposition of procedures for such a model type.
The authors of [13] researched the impact of fillet welds caused by the increased surface of the brace member cross section in the joint zone on rectangular hollow section "T" joints. The behaviour of joints with various geometries and dimensions of the fillet weld was analysed. The study proposed an increase in the brace member cross-section, which would make the results of the joint calculation more approximate and realistic joint behaviour.
In [14], the authors numerically investigated the static strength of steel-collar-plate-reinforced tubular T/Y joints. The researchers demonstrated that the strength of joints reinforced with steel collars is higher than that of non-reinforced joints and proposed a new equation for determining the ultimate strength of collar plate-reinforced "T"/"Y" joints under axial compressive loads.
In [15], the behaviour of different shapes of CHS and RHS "Y" joints was analysed. Using the finite element method, the authors derived equations to determine the stress concentration factor.
Another group of authors, using non-linear analysis with FEM for determining the ultimate load-bearing capacity of "Y" joints [16], concluded that the variation of geometrical parameters of the joint considerably affects joint behaviour. They paid particular attention to weld modelling, i.e. density of the finite element mesh in the proximity of seams, which, due to their function, are located at locations where sudden changes in force flow and stress concentration occur. The authors provided recommendations for forming a finite-element mesh in the weld zone.
In [17], the authors described methods for designing precise geometric and finite-element models for tubular Y-joints with cracks. The methods were proposed to model cracks at any location at the intersection of the chord and brace members, as well as to generate a finite element mesh of Y joints with and without damage.
Paper [18] shows the modelling techniques used in finite element analysis to obtain information on the strength, load zones, and load intensity factors. In addition, guidelines on the discretisation of models, choice of elements, material curve application, result interpretation, and numerical techniques have limitations.
In [19], a non-linear finite element simulation based on a parametric study was conducted to analyse tubular joints, considering the weld geometry, material, and geometrical nonlinearities. The authors of this study analysed the behaviour of the brace-to-chord width ratio and thickness-to-chord face width ratio.
Reference [20] dealt with the numerical modelling of the Y joints of HSS truss beam elements. The authors presented the obtained results, selected the non-linear numerical analysis parameters, and laid out the practical conclusions used in this study.
Researchers have also aimed to determine the effects of material properties [21]. Considering that researchers often use a simplified stress–strain diagram (bilinear diagram), the authors presented limitations to such an approach in their study.

3. Directly welded joints of steel truss beams – general points

Unlike traditional joints realised using gusset plates, the joints of directly welded elements of truss beams made of hollow sections require different approaches during construction and design. The results of research in this area, which are based on the limit state theory, show that the behaviour of such joints does not depend only on the quality of the base material, the geometric characteristics of the joint elements, and the shape and intensity of the load in the chord members of the beam, but also on the construction of the joint, that is, its shape. The derived equations determining the bearing capacity of the given joints for each potential failure mode are presented as a function of the maximum bearing capacity of the brace elements under the effect of the axial force and/or bending moment. Limitations regarding the relationships of the geometric characteristics of the joint elements, that is, the area of validity, are also defined, which fulfil the conditions of the serviceability limit state and are reflected in the form of limitation of local deformations at the joint, as well as prevention of reduction in the capacity of rotation and/or deformation. All joint resistance equations were proven experimentally within the defined ranges of validity. In cases of exceeding the joint strength and when it is not possible to change the defined cross-sections of the truss beam elements, reinforcing the joint depending on the failure mode is necessary.

Figure 1 shows some (T, X, Y joints) of multiple types of plane joints of hollow structural section truss beams according to EC 3.

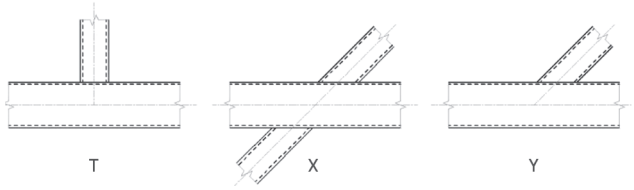

Figure 1. Types of joints of truss beams made of hollow sections [3]

A failure criterion based on the serviceability limit state value was determined based on numerous numerical and experimental studies, which is important for determining the ultimate strength of RHS or CHS joints, where the stress-strain curve, that is, moment rotation, does not exhibit a precise value for the ultimate force. In the studies [11, 22-27], the ultimate value of deformation is defined, which is 3 % of the width () / height () to which corresponds the ultimate joint resistance, as shown in Figure 2 in P-Δ (force – strain) diagram.

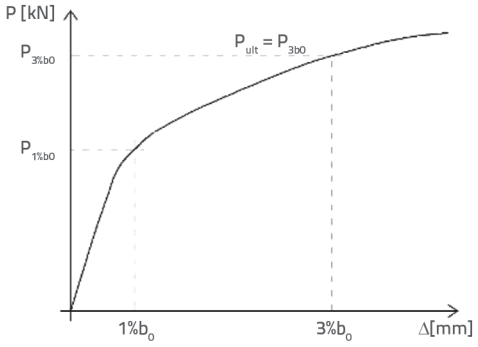

Figure 2. Ultimate joint strain

Based on the experimental research conducted by Wardenier and Stark in 1978 and Kurobane in 1980/81 and in relation to the behaviour of joints of directly welded elements of truss beams made of hollow sections, the basic failure modes of the joints [3] were formed (Figure 3), on which the design resistances of hollow section joints are based.

4. Numerical and experimental analysis of ultimate resistance of steel "Y" joint with damage

This study investigated the effects of damage to a brace member on the resistance of a Y-joint made of directly welded rectangular hollow sections under axial force action. Cold-formed resistance S235JR steel sections are selected for the numerical and experimental tests. The chord member was made of SHS 80 × 80 × 3, and the brace member was made of SHS 50 × 50 × 4. The brace member is set at an angle of 45° relative to the chord member. The chord and brace members were welded with fillet welds 3 mm thick. The lengths of the chord and brace members were 400 and 200 mm, respectively.

	Failure mode	Axial load
(a)	Chord face failure (plastic failure of the chord face) or chord plastification (plastic failure of the chord cross-section)	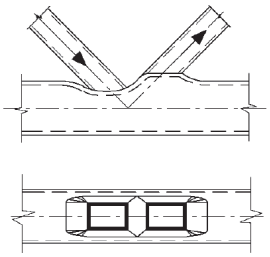
(b)	Chord side wall failure (or chord web failure) by yielding, crushing or instability (crippling or buckling of the chord side wall or chord web) under the compression brace member	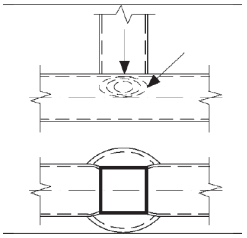
(c)	Chord shear failure	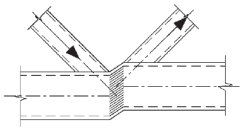
(d)	Punching shear failure of a hollow section chord wall (crack initiation leading to rupture of the brace members from the chord member)	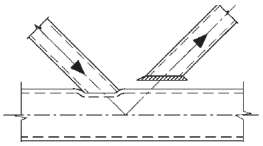
(e)	Brace failure with reduced effective width (cracking in the welds or in the brace members)	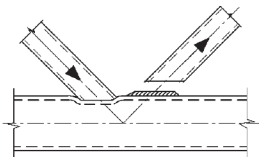
(f)	Local buckling failure of a brace member or of a hollow section chord member at the joint location	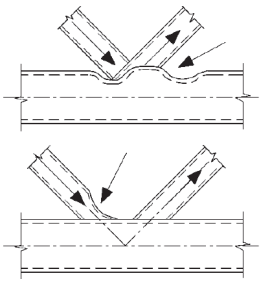

Figure 3. Failure modes of joints of brace members and rectangular hollow section chords [3]

Figure 4 shows the geometry of the joint without damage. This research aimed to establish the extent to which the damage and its propagation in the chord member affect the ultimate resistance of the joint compared to a joint without damage. The subject of this research was the propagation of damage in the vertical direction; that is, the height of the damage increased, whereas the width of

the damage was unchanged. For this purpose, the results of the undamaged and damaged specimens were compared (Figure 5 and Table 1) using the finite element method (FEM). The chosen damage was in the form of cracks (simulated as narrow rectangles) and was positioned on both sides of the chord member beneath the joint of the brace and chord elements.

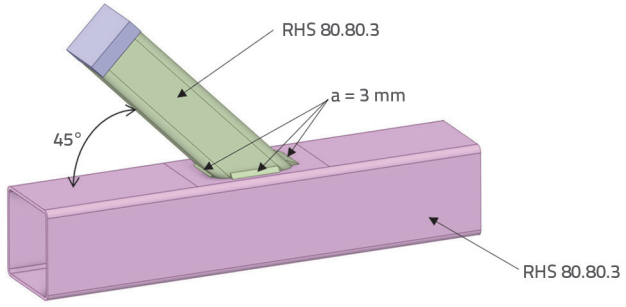

Figure 4. Geometry of the specimen without damage (Y-joint_ND)

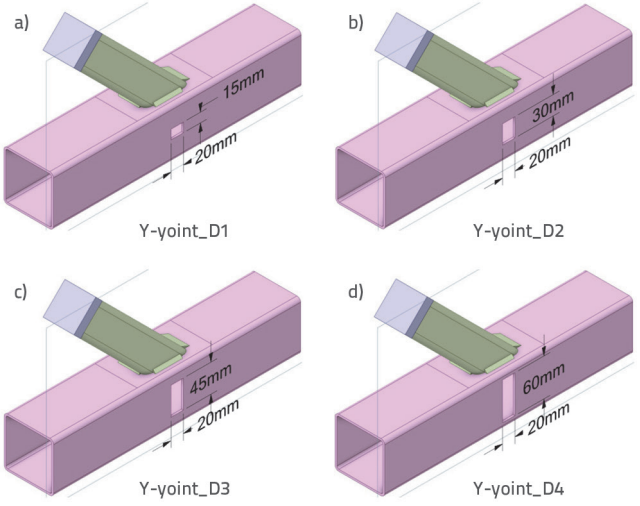

Figure 5. Analysed specimens with damage on the sides of the chord member

4.1. Numerical analysis

The numerical analysis considered both the joint without damage and the joints with varying percentages of damage (9.55 %,19.10 %, 28.66 %, and 38.21 %). The damage sizes on both sides of the chord members are presented in Table 1. The design model was modelled using the finite element method in the ANSYS software package [28]. The analysis included both geometric and material nonlinearities. The joint was modelled as a joint of two solid bodies. The chord and brace members were modelled as two independent bodies. These two elements were joined by fillet welds 3 mm thick. For simplicity, only the straight parts of the welds on the contact between the chord and brace sections were modelled, whereas the circular part was not. Another solid body was modelled at the free end of the brace element. This solid body simulates the spherical element used to transmit the force to the brace element. To achieve a sufficiently high stiffness, the adopted material of the spherical element had 1000 times higher modulus of elasticity and material strength values than that of the joint elements. The boundary conditions (Table 2 and Figure 6) and contact conditions (between the sphere plate and diagonal brace section, diagonal brace section and welds, and welds and chord section) were modelled to simulate the experimental conditions realistically.

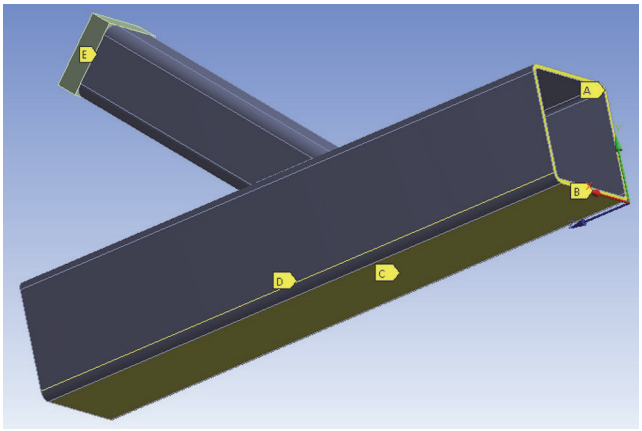

Figure 6. Boundary conditions

Table 1. Analysed specimens

Specimen	Size of the damage on both sides	Percentage of cross-section damage [%]
Without damage (Y-joint_ND)	-	0
Damage 1 (Y-joint_D2)	15 x 20 mm	9.55
Damage 2 (Y-joint_D2)	30 x 20 mm	19.10
Damage 3 (Y-joint_D3)	45 x 20 mm	28.66
Damage 4 (Y-joint_D4)	60 x 20 mm	38.21

Table 2. Boundary conditions

Explanation of Figure 6	Element type	Prevented displacement
A	Area support	Z = 0
B	Linear support	X = Y = Z = 0
C	Area support	Y = 0
D	Linear support (both sides of chord member)	X = 0
E	Point support (the middle of the upper surface of the solid plate)	Load as node displacement Y = Z = 6 mm

Table 3. Characteristics of the material adopted for the numerical analysis

Element	f_y [MPa]	f_u [MPa]	E [MPa]
SHS 80x80x3	361	402	207400
SHS 50x50x4	410	430	201600

The contacts between the chord member and fillet welds, the fillet welds and brace member, and the brace member and rigid body were modelled using the bonded contact pair between the surfaces of the body faces. The material in the model corresponds to the material on which the experimental test was performed (Table 3). The fields were modelled with the same material characteristics as the brace member (SHS 50x50x4). The non-linear behaviour of the steel was modelled using multilinear isotropic hardening. The stress-strain curve slope between the yield point (fy) and tensile strength (fu) was adopted as 1 % of Young's modulus of elasticity (E). After reaching the tensile strength, the adopted material was considered ideally plastic.

The finite element mesh was modelled using a generator in the software package. In the high-stress concentration areas, on the top flange of the chord element, the finite element mesh was made denser (the finite elements were twice as small as the finite elements on other parts of the model) (Figure 7). The mesh was formed using SOLID187 elements, a higher 3-D order of elements with 10 nodes, and the square behaviour of the displacement, which is suitable for modelling irregularly shaped meshes. The research of the authors in [20] on a Y-joint showed that mesh elements smaller than 10 mm did not yield more precise results (Figure 8). Therefore, in this study, when modelling a joint with and without damage, a mesh with 10 mm elements was adopted, 5 mm in the denser zone (top flange of the chord element).

An axial compression force was imparted to the diagonal joint element by displacing the central point of the spherical joint solid plate.

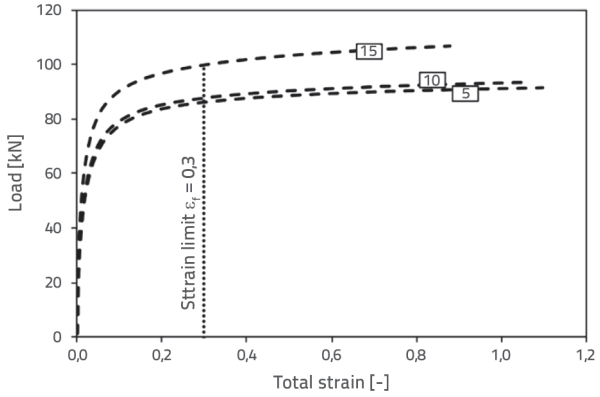

Figure 8. Mesh convergence study [20]

Table 4 lists the values of the ultimate joint resistance obtained using the numerical FEM analysis.

Table 4. Ultimate joint resistances obtained using FEM

Specimen	Ultimate resistance [kN]
Without damage (Y-joint_ND)	86.4
Damage 1 (Y-joint_D1)	86.2
Damage 2 (Y-joint_D2)	86.0
Damage 3 (Y-joint_D3)	84.5
Damage 4 (Y-joint_D4)	79.8

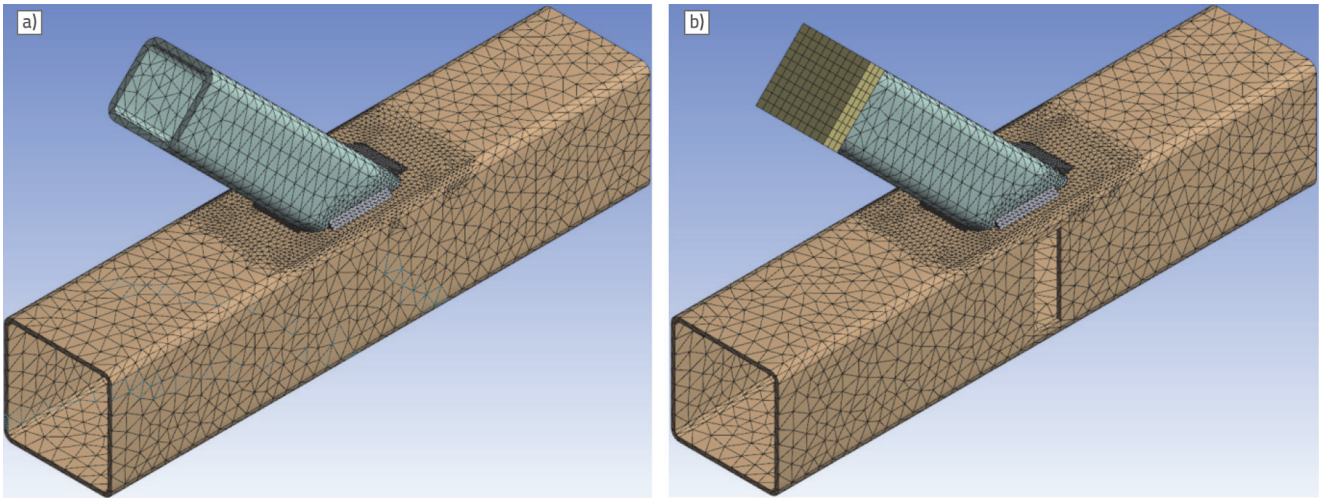

Figure 7. a) Finite element mesh of the joint without damage; b) the joint with the highest damage percentage

As expected, the results of the numerical analysis showed that with the occurrence and further propagation of damage, there was a decline in the ultimate resistance of the joint. The ultimate resistance of the joint is determined, in compliance with the recommendations of IIW (International Institute of Welding), at the strain amounting to (Figure 9). This recommendation is the result of experimental tests that prove that when controlling the joint resistance, the limit state of serviceability is irrelevant; that is, no cracks occur during the operation of the structure.

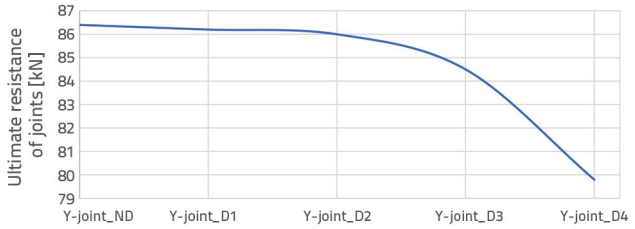

Figure 9. Diagram of ultimate resistance depending on the degree of damage

Figures 10, 11, and 12 provide the diagrams of the point displacement on the side wall of the chord member, on the side of the top flange and on the top flange of the chord member in front of the brace member, determined by FEM, for the cases of the specimen without damage and specimens with (9.55 %, 19.10 %, 28.66 % and 38.21 %).

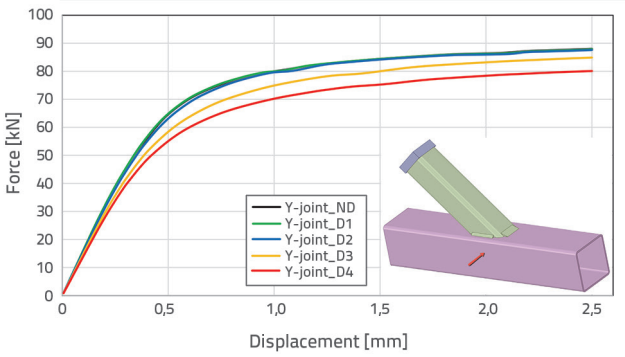

Figure 10. Numerically obtained diagrams of force vs point displacement of the side wall of the chord member

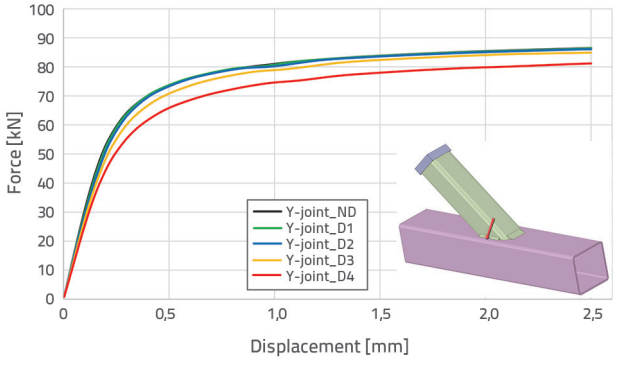

Figure 11. Numerically obtained diagrams of force vs point displacement on the top flange of the chord member on the side of the brace member

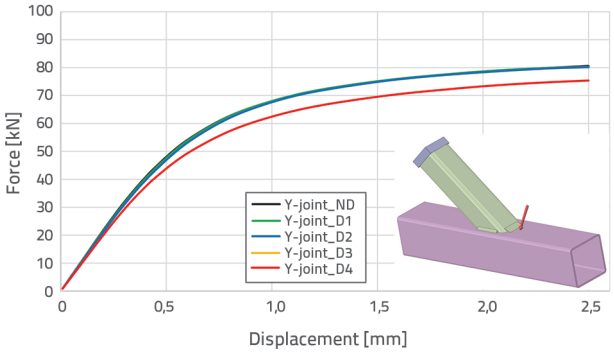

Figure 12. Numerically obtained diagrams of force vs point displacement on the top flange of the chord member in front of the brace member

The results indicate that with an increase in the damage percentage, the same values of the characteristic point displacement occur at lower intensities of the axial forces; that is, the lower the damage percentage, the lower the point displacement.

4.2. Experimental analysis

Experimental tests were conducted on specimens without damage, two types of specimens with damage, one specimen with 19.10 % damage (Y-joint_D2), and one specimen with 38.21 % damage (Y-joint_D4) (Figure 13).

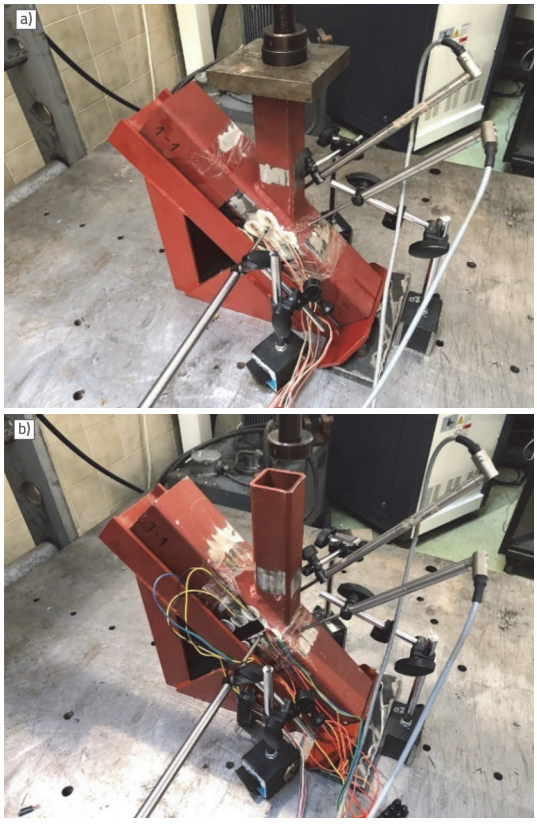

Figure 13. Specimen test: a) without damage (Y-joint_ND), b) with damage 4 (Y-joint_D4)

The test was performed using a hydraulic press with a capacity of 100 tons at the Laboratory of the Faculty of Mechanical Engineering of Nis.

The following measuring equipment was used to register and record the results (all equipment was manufactured by Hotinger Baldwin Messtechnik).

- Measuring cells of displacement (travel) WA 100, WA 50, and WA 20
- force measuring cell Z4A 100 kN
- strain gauges LY 41 – 6 mm 700 Ω and LY 21 – 1.5 mm 120 Ω. The measuring gauges were glued using a two-component glue X60
- switch for strain gauges for individual static measuring of stress at one measuring point
- amplifier Quantum MX 840.

For the test, the chord member of the joint was set at an angle of 45° relative to the horizontal plane, which allowed the hydraulic press to impart an axial force to the diagonal member. To avoid the eccentric transmission of force to the diagonal member, the load was transmitted via a spherical element set between the diagonal member and the press. The load is applied in the prescribed range defined by EN ISO 6892-1 [29].

The strain gauges were arranged according to the space available for mounting on the measuring point and the expected strain of the observed points on the chord element:

- strain gauges LY 41 – 6 mm 700 Ω – positions 11, 12, 13, 14, 15, 16, 21, 22, 23, 24, 25, 26, 27, 28, 31, 32, 33, 34, 35, and 36;
- strain gauges LY 21 – 1.5 mm 120 Ω – positions 29, 210, 37, 38.

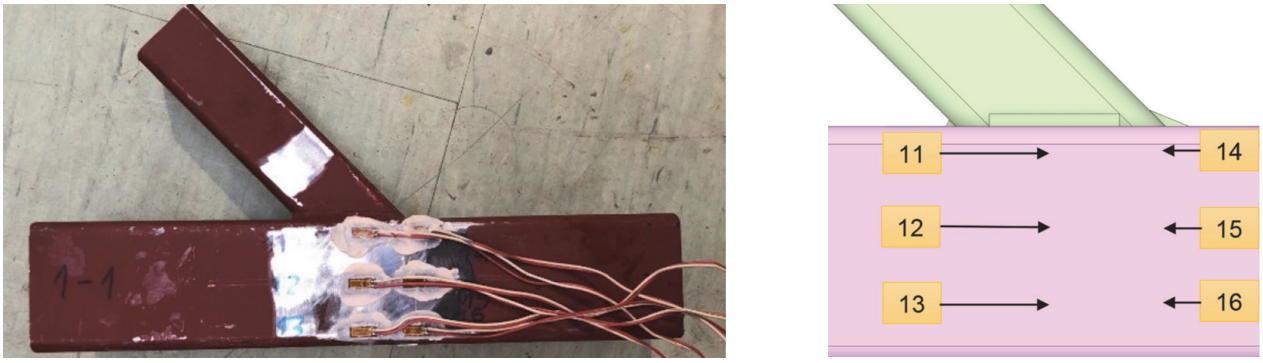

Figure 14. Arrangement of strain gauges on the specimen without damage (Y-joint_ND)

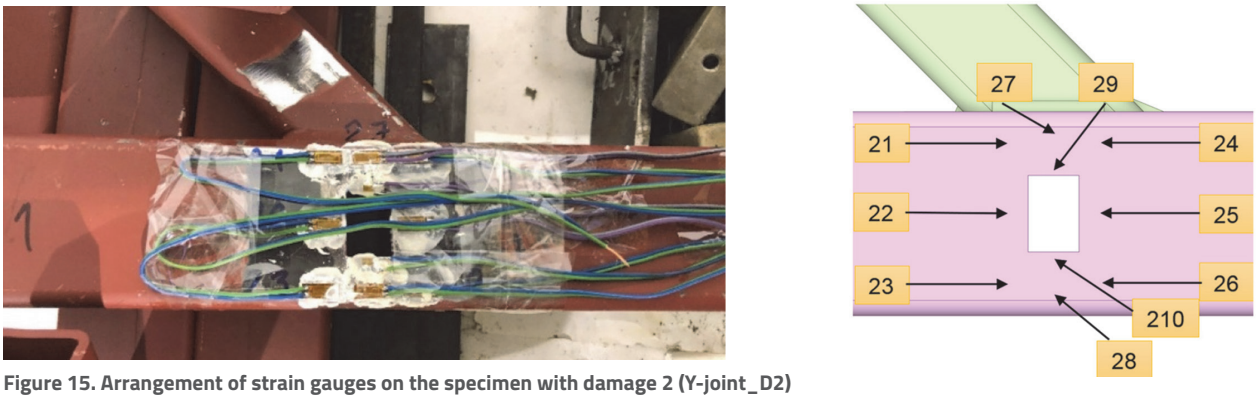

Figure 15. Arrangement of strain gauges on the specimen with damage 2 (Y-joint_D2)

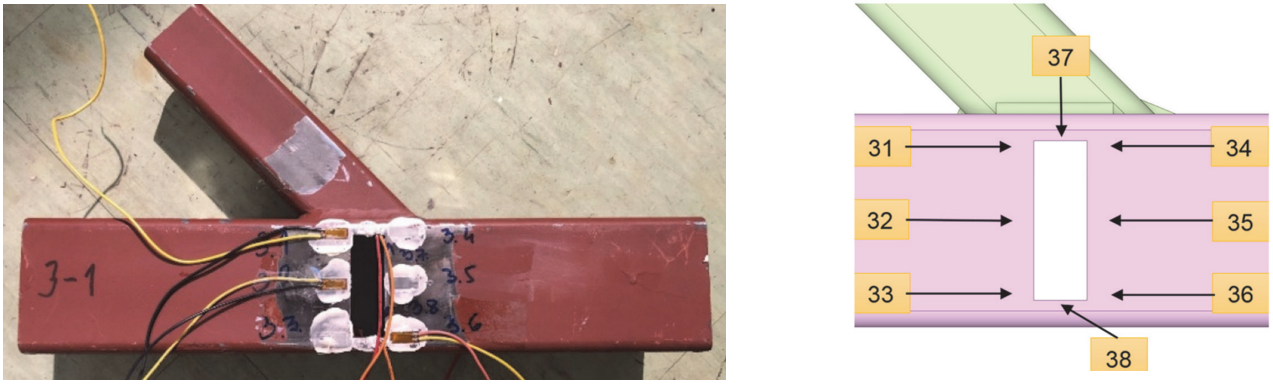

Figure 16. Arrangement of strain gauges on the specimen with damage 4 (Y-joint_D4)

Figures 14, 15, and 16 show the arrangement of the strain gauges on the model without damage (Y-joint_ND) and on damaged models 2 (Y-joint_D2) and 4 (Y-joint_D4), respectively. Figure 17 shows the arrangement of the measuring instruments and strain gauges on an undamaged specimen (Y-joint_ND).

Figures 18, 19, and 20 provide the experimentally obtained force–displacement diagrams of the characteristic points where the highest strain occurred.

By observing the diagrams in Figures 18, 19, and 20, it can be concluded that at the designated points (point at the side wall of the chord member, point on the top flange of the chord member on the side of the brace member, and point on the top flange of the chord member in front of the brace member) at the same force, the observed model has a higher deformation with more significant damage, that is, the ultimate resistance decreases with the increase in damage size.

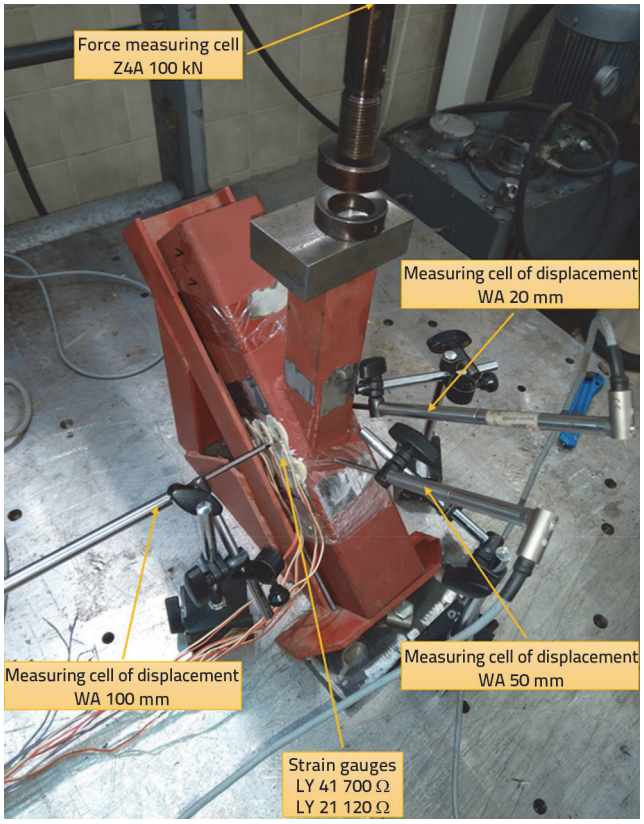

Figure 17. Arrangement of measuring instruments and strain gauges on the specimen without damage (Y-joint_ND)

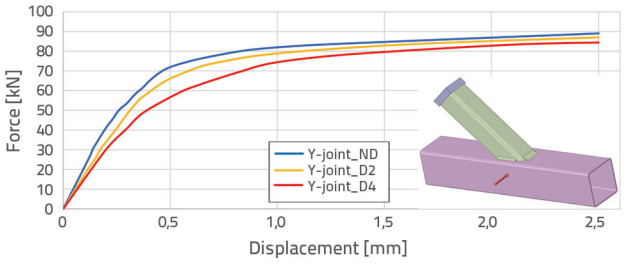

Figure 18. Experimentally obtained diagrams of the point displacement on the chord member side

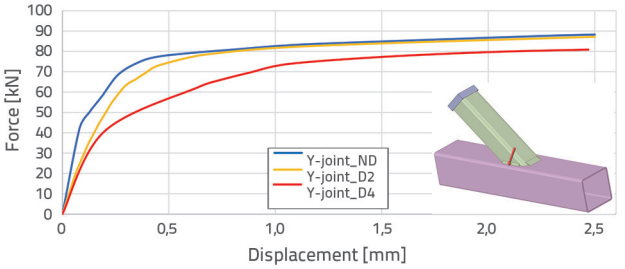

Figure 19. Experimentally obtained diagrams of the point displacement on the top flange of the chord member on the side of the brace member

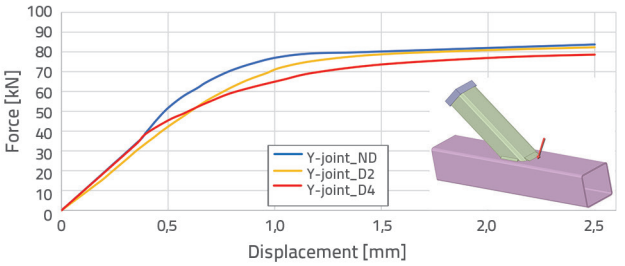

Figure 20. Experimentally obtained diagrams of the point displacement on the top flange of the chord member in front of the brace member

5. Discussion

Figures 21, 22, and 23 provide comparative diagrams of the displacement of the characteristic points in which the highest strain is expected, as obtained by the finite element method and experiments.

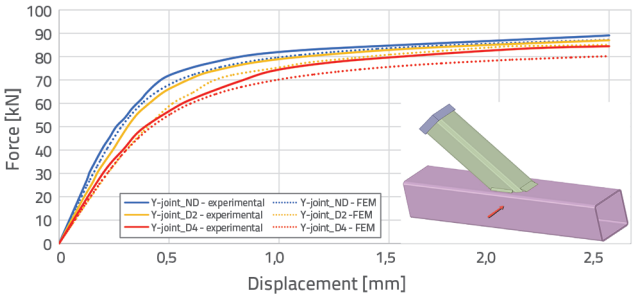

Figure 21. Comparative diagrams of the point displacement on the chord member side

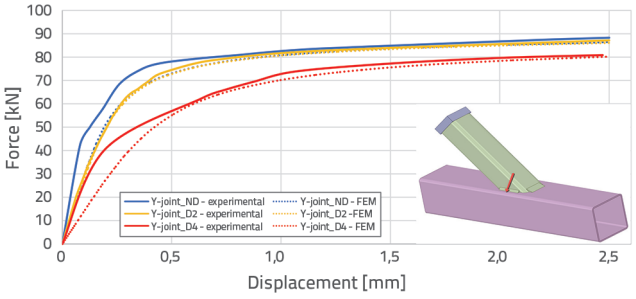

Figure 22. Comparative diagrams of the point displacement on the top flange of the chord member on the side of the brace member

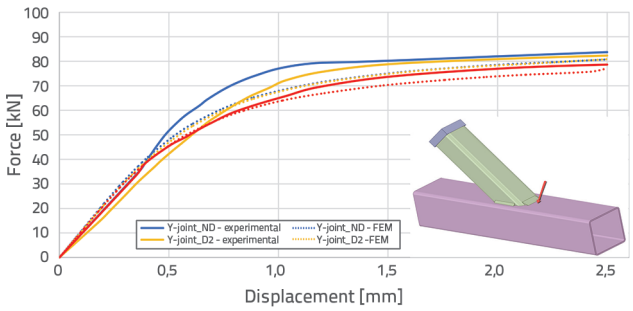

Figure 23. Comparative diagrams of the point displacement on the top flange of the chord member in front of the brace member

This paper presents the results of numerical and experimental research on the directly welded Y joint of the SHS chord and diagonal members with damage in the joint in the form of a narrow vertical rectangular crack. This damage propagates along the height of the chord until reaching its final, as well as the joint with elements without damage. The numerical research results using the finite element method and experimental research were in reasonable agreement. The deviation of the results obtained by the numerical and experimental procedures was, on average, 3 to 5 %.

The experimental data confirm the numerically obtained results. With increasing damage, the joint elements had a higher strain at the same axial force intensities, that is, a decline in the ultimate resistance. The point displacement, that is, the joint strain in the experimental research, occurred at higher intensities of the axial force. The shape of the diagram of the experimental results coincides with the shape of the diagram of the numerically obtained results, with slightly higher axial force intensities.

6. Conclusion

This study employs the FEM to analyse the complex state of stress and deformation at the truss node, which is not always possible when using analytical methods. The experimental analysis confirmed the calculation results for a specific number of adopted parameters of the chosen FEM model.

The ultimate resistance of the joint was achieved because of the exhaustion of the local plasticisation of the chord element surface (failure modes (a) and (b), according to Table 3 [3]).

No cracks were detected in the joint zones with the most significant deformation during the tests.

The research revealed the dependence of the ultimate resistance and degree of damage owing to damage propagation, which facilitated the assessment of the load-bearing capacity of the structure during the monitoring of the structural status.

Based on the results of the numerical and experimental analyses, it was concluded that with an increase in the damage to the chord element of the joint, the ultimate resistance of the joint declined in a non-linear fashion. The decline in the ultimate resistance of specimens with damage of 9.55 % and 19.10 % is negligible, amounting to cca 0.5 %, whereas for the tested samples having a chord member cross-section damage of 38.21 %, the decline in the ultimate resistance of the joint was cca 8 %, which reveals the good behaviour of the joint for the chosen damage.

REFERENCES

[1] Milošević, M., Živković, S.: Rešetkasti nosači bez čvornih limova od šupljih čeličnih profila, Zbornik radova Građevinsko-arhitektonskog fakulteta, 31 (2016) 16, pp. 92-111.

[2] EN 1993-1-1 – Eurocode 3 – Design of steel structures – Part 1-1: General rules and rules for buildings.

[3] EN 1993-1-8 – Eurocode 3 – Design of steel structures – Part 1-8: Design of joints.

[4] Dobrić, D.J.: Analiza ponašanja čvorova rešetkastih nosača od šupljih profila, magistarski rad, Građevinski fakultet Univerziteta u Beogradu, 2007.

[5] Wardenier, J., Kurobane, Y., Packer, J.A., Van der Vegte, G.J., Zhao, X.L.: Design guide for circular hollow section (CHS) joints under predominantly static loading, CIDECT, TUV-Verlag, 2008.

[6] Zhao, X.L., Herion, S., Packer, J.A., Puthli, R.S., Sedlacek, G., Wardenier, J., Yeomans, N.F.: Design guide for circular and rectangular hollow section welded joints under fatigue loading, CIDECT, TUV-Verlag, 2001.

[7] Zhao, X.L., Wardenier, J., Packer, J.A., Vegte, G.V.D.: Current static design guidance for hollow-section joints, Proceedings of the Institution of Civil Engineers-Structures and Buildings, 163 (2010) 6, pp. 361-373, https://doi.org/10.1680/stbu.2010.163.6.361

[8] Lan, X., Chan, T.M.: Recent research advances of high strength steel welded hollow section joints, Structures, 17 (2019), pp. 58-65, https://doi.org/10.1016/j.istruc.2018.11.015

[1] Živković, S.: Doprinos proračunu direktno zavarenih veza elemenata rešetkastih nosača od šupljih čeličnih profila pravougaonog i kvadratnog poprečnog preseka, doktorski rad, Građevinsko-arhitektonski fakultet, Univerziteta u Nišu, 2014.

[10] Yang, D.P., Shao, Y.B., Long, F.L., Niu, G.Q., Zhang, L., Zhi, J.B.: Static strength of RHS T-joints with reinforced chord under in-plane bending load, Applied Mechanics and Materials, Trans Tech Publication Ltd., 488 (2014), pp. 790-794, https://doi.org/10.4028/www.scientific.net/AMM.488-489.790

[11] Garifullin, M., Pajunen, S., Mela, K., Heinisuo, M.: Finite element model for rectangular hollow section T joints, Rakenteiden Mekaniikka (Journal of Structural Mechanics), 51 (2018) 3, pp. 15-40, https://doi.org/10.23998/rm.70439

[12] Garifullin, M., Pajunen, S., Mela, K., Heinisuo, M.: 3D component method for welded tubular T joints, Tubular Structures XVI: Proceedings of the 16th International Symposium for Tubular Structures, pp. 165-173, 2017. https://doi.org/10.1201/9781351210843-20

[13] Bronzova, M., Garifullin, M., Mela, K.: Influence of fillet welds on structural behavior of RHS T joints, International Symposium on Tubular Structure, pp. 590-597, 2019. https://doi.org/10.3850/978-981-11-0745-0 055-cd

[14] Nassiraei, H., Lotfollahi-Yaghin, M.A., Ahmadi, H.: Static strength of collar plate reinforced tubular T/Y-joints under brace compressive loading, Journal of Constructional Steel Research, 119 (2016), pp. 39-49, https://doi.org/10.1016/j.jcsr.2015.12.011

[15] Yin, Y., Lui, X., Lei, P., Zhou, L.: Stress concentration factor for tubular CHS-to-RHS Y-joints under axial loads, Journal of Constructional Steel Research, 148 (2018), pp. 768-778, https://doi.org/10.1016/j.jcsr.2018.06.003

[16] Wang, Y.Q., Jiang, Y., Shi, Y.J., Sun, P.: Non-linear analysis of ultimate loading capacity of cast tubular Y-joints under axial loading, Tubular Structures XII Proceedings of the 12th International Symposium on Tubular Structures, Shanghai, China, pp. 529-532., 2008.

[17] Lie, S.T., Lee, C.K., Wong, S.M.: Model and mesh generation of cracked tubular Y-joints, Engineering Fracture Mechanics, 70 (2003) 2, pp. 161-184, https://doi.org/10.1016/S0013-7944(02)00036-X

[18] Lee, M.M.K.: Strength, stress and fracture analyses of offshore tubular joints using finite elements, Journal of Constructional Steel Research, 51 (1999) 3, pp. 265-286, https://doi.org/10.1016/S0143-974X(99)00025-5

[19] Bittencourt, M.C., Lima, L.R.O., De Vellasco, P.C.G.S., Silva, J.G.S., Neves, L.G.C.: A numerical analysis of tubular joints under static loading, Proceedings of APCOM'07 in conjunction with EPMESC XI, Kyoto, Japan, 2007.

[20] Živković, S., Stojković N., Turnić, D., Milošević, M.: Numerical modelling of Y joints of trusses made of steel hollow sections, Tehnički vjesnik / Technical Gazette (TV/TG), 27 (2020) 6, pp. 2083-2088, https://doi.org/10.17559/TV-20190513073712

[21] Pelletier, H., Krier, J., Cornet, A., Mille, P.: Limits of using bilinear stress-strain curve for finite model element modeling of nanoindentation response on bulk materials, Thin Solid Films, 379 (2000) 1-2, pp. 147-155, https://doi.org/10.1016/S0040-6090(00)01559-5

[22] Packer, J.A., Wardenier, J., Kurobane, Y., Dutta, D., Yeomans, N.: Design Guide for Rectangular Hollow Section (RHS) Joints Under Predominantly Static Loading, The International Committee for the Study and Development of Tubular Structures, Köln, Germany 1992.

[23] Lu, L.H., de Winkel, G.D., Wardenier, Yu, Y.: Deformation limit for the ultimate strength of hollow section joints, Proceedings of the Sixth International Symposium on Tubular Structures, Melbourne, Australia, 1994.

[24] Lu, L.H.: The static strength of I-beam to rectangular hollow section column connections, PhD thesis, Delft University Press, Delft, The Netherlands, 1997.

[25] De Winkel, G.D.: The static strength of I-beam to circular hollow section column connections, PhD thesis, Delft University Press, Delft, The Netherlands, 1998.

[26] Zhao, X.L.: Deformation limit and ultimate strength of welded T-joints in cold-formed RHS sections, Journal of constructional steel research, 53 (2000) 2, pp. 149-165.

[27] Kosteski, N., Packer, J.A., Puthli, R.S.: A finite element method based yield load determination procedure for hollow section connections, Journal of Constructional Steel Research, 59 (2003) 4, pp. 453-471.

[28] ANSYS – Software manual.

[29] EN ISO 6892-1:2020: Metallic materials – Tensile testing – Part 1: Method of test at room temperature (ISO 6892-1:2019).